Crash and Durability of Aluminum and Mixed Steel Aluminum Joints Made by Electromagnetic Pulse Welding

F. Huberth[1*], S. Klitschke[1], M. Gall[1], S. Sommer[1], K. Schnabel[2], J. Baumgartner[2],

[1] Fraunhofer Institute for Mechanics of Materials IWM, Freiburg, Germany;
[2] Fraunhofer Institute for Structural Durability and System Reliability LBF, Darmstadt, Germany
*Corresponding author. Email: frank.huberth@iwm.fraunhofer.de

Abstract

In this paper, results of the research project "Failure behavior of mixed weld joints under multi-axial crash-like and cyclic loads on the example of EMPT sheet metal joints" funded by the German Federal Ministry for Economic Affairs and Energy are presented and discussed. Aluminum and mixed aluminum-steel joints were prepared using electromagnetic pulse technology (EMPT) at PSTproducts GmbH (PST). Investigations on coupon samples were performed under oscillating and monotone (crash) loadings until failure. Based on the coupon tests, parameters for modelling the crash performance were derived, using both a detailed continuum model and an application driven simplified FE-model. The derived FE-modelling concept for crash behavior was validated by comparison of component tests and simulations Durability analysis of the joint specimens was performed combined with FEM analysis, applying the notch stress concept. For the notch stress concept a notch model with a reference radius of r_{ref}=0.05 mm was used for the FE-simulations. The endurable notch stresses were compared to reference S-N curves derived for conventional welded samples. The EMPT-results fit well in the scatter band of the conventional laser-welded joints. This is the verification that the notch stress concept can be successfully applied also for EMPT joints.

Keywords

Joining, Electroforming, Crash and Durability

1 Introduction

The project was motivated by the demand for mixed (hybrid) joining of metal lightweight automotive components. Many mixed joining technologies reduce the performance of the components beneath the level of the weakest part in the load path. This is well investigated in Meschut, G., Janzen, V. & Olfermann, T. (2014). They show that a welding process outperformed the other processes. The friction element welding (FEW) connection of metal sheets reported by Meschut et al. shows a maximum load of 9 kN during lap shear tests compared to less than 7 kN for high speed tack joining (RIVTAC®), clinching and other processes. They show also the combined results of different joining processes combined with adhesive bonding. The pure adhesive bonding showed the best performance with a maximum load of 19.59 kN compared to 18.06 for FEW combined with adhesive bonding. Combining the advantages of distributed force transmission which is characteristic of adhesive bonding with the processing speed of the dynamic welding process, the EMPT-joining process - so named by PST and in this paper , more generally known as magnetic pulse welding (MPW) - promised to provide both, good load bearing capacity as well as short processing interval. The MPW process uses electromagnetic forces to accelerate a section of a metal sheet, the so called “flyer”, onto a stiff or supported target surface. The resulting high speed impact achieves a solid state welding. This avoids the process heat introduced weakening of the joint area which is typically encountered in standard welding processes. More details on MPW are given e.g. by Kang (2015).
As reference joint an aluminum-aluminum combination was chosen using EN-AW 6016 in T4 for joining, followed by a simulation of the paint bake process at 185°C for 20 minutes. For the main aim of the project the combination of an EN-AW-6063 and a DP1000 steel (HCT980X) was chosen and with this combination the final assembly of a T-joint component was realized. The steel was chosen in a nongalvanized variant, to avoid the influence of the coating or a devarnishing. The T-joint component represents a showcase that can be directly transferred to an industrial application like a mixed material space frame. A good example for such an aluminum-steel mixed construction is the actual Audi A8 space frame. The amount of aluminum for the A8 car body is about 58% and about 40% of steel (Poll, D. 2017). A full overview about the project is given in the final project report (Huberth, F., Baumgartner, J., 2017).

2 Sample Preparation with EMPT

The joint samples and the T-joint components were prepared at PST. The EMPT process was defined with an overlapping position of the coil as shown in the sketch in **Fig. 1**.
The three different combinations, which were realized, are shown in **Fig. 2**. The first two samples were prepared without a driver sheet; the third one at the right shows a sticking rest of the driver used there for joining.

Figure 1: *Setup of the EMPT-process for aluminum samples (left) and mixed aluminum-steel samples with an additional aluminum driver (right)*

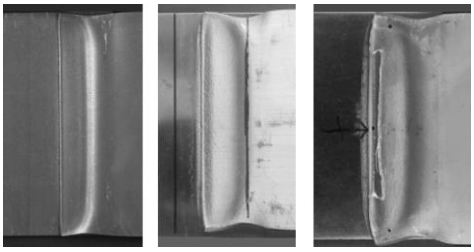

Figure 2: *Lap-shear sample for the configurations: EN-AW 6016 with EN-AW 6016 flyer, left, HC420LA with EN-AW 6063 flyer, center, DP 1000 with EN AW-6063 flyer at the right*

3 Experimental Investigations

3.1 Base Materials Characterization

The base materials of the coupon samples were investigated in tensile, notched tensile and shear tests at different nominal strain rates to include strain rate effects on the materials in the crash-simulations.
All used materials showed a rate effect from very low stress hardening of about 10 MPa for the EN-AW 6016 and an increased failure strain with increasing strain rate in tensile tests up to an increased maximum load for EN AW-6063 from 140 MPa for a quasi-static load up to 180 MPa for a dynamic load with a nominal strain rate of 250 s^{-1}.
For the DP 1000 steel the tensile strength R_m increased from 1000 MPa at quasi-static load up to 1140 MPa at a nominal strain rate of 100 s^{-1} (Huberth, F., Baumgartner, J. 2017).

3.2 Experimental Investigations of the Aluminum Joints under monotone (Crash-) Loads

The EN-AW 6016- EN-AW 6016 samples were tested in lap-shear and peel test. First lap-shear tests showed a strong influence of the lateral end areas of the joint (**Fig. 3, A**) on the failure behavior. Initialization of the sample failure in the lateral end areas of the joint was verified for quasi static loads at 0.02 mm/s elongation (**Fig. 3, B**). For dynamic (crash) loads at an elongation speed of 3 m/s, the failure mode changed and was initialized in the sample center, (**Fig. 3, C and D**). The dynamic loading on the sample was initiated at a servo hydraulic testing machine after an acceleration phase using a slack adapter. For well-

defined parameter identification for simulation lap-shear tests were carried out on waisted samples where the radial end areas on both sides of the joint were cut off (**Fig. 3, E**). These tests were performed for 20 mm and 30 mm width of the resulting joint area, leading to comparable results, normed on the width. For this configuration no loading velocity dependence in the failure mode was observed. One example for 30 mm width samples is shown in **Fig. 3 E**.

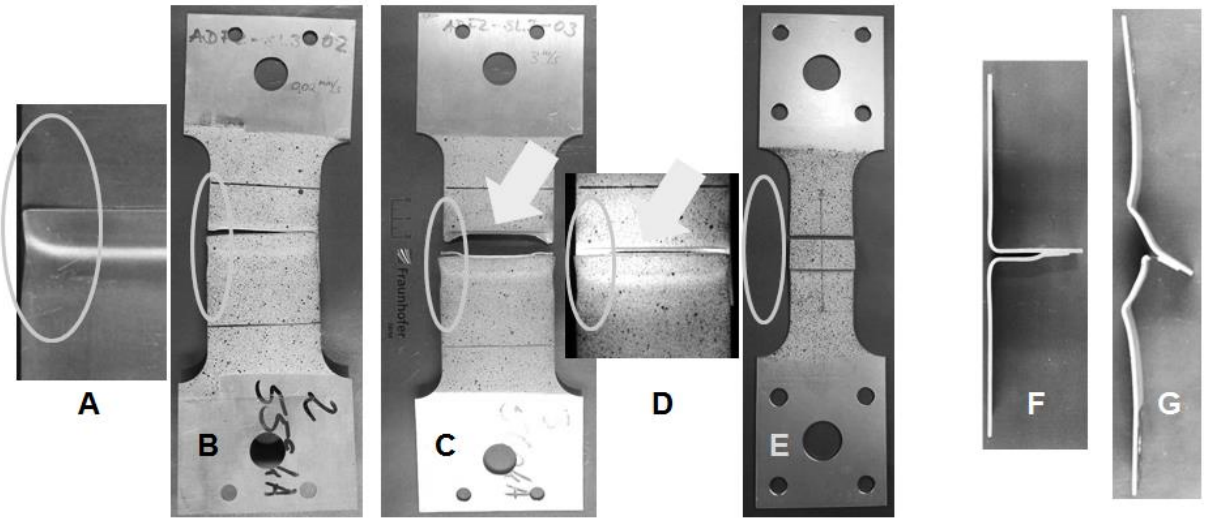

Figure 3: *Lap-shear samples (A-E) with optimized geometry and full welding zone (B and C), detail (A) with marked lateral end areas of the joint (A-E), sample failed under quasi static load (B), and dynamic load of 3 m/s, (C and D) with failure initialization detail (D); a tested waisted sample is shown in E, without the lateral end areas; bended peel test samples before (F) and after testing (G)*

Based on these results all peel test samples were cut in width, to avoid influence of the lateral end areas of the joint. Peel samples were prepared by EMPT joining of two straight sheets at one end, followed by bending the long ends of the sheets away in a 90° angle. A bended sample is shown before (**Fig. 3 F**) and after testing (**Fig. 3 G**).
The tailored lap-shear tests were mainly used for parameter identification for the simulation. Adaption of the influence of the lateral radial end areas of the joint was based on these results and on results of tests with the full welding zone samples. The peel test failure was mainly driven by the local deformation directly before the welding zone, as can be seen in **Fig. 3 G**.

3.3 Experimental Investigations of the mixed Steel-Aluminum Joints under monotone (Crash-) Loads

The tests for the mixed material joints showed a mixed failure behavior, too. Different failure modes occurred during the quasi-static lap-shear tests (**Fig. 4, A and B**) and the peel tests. For the dynamic tests at 3 m/s the lap-shear samples failed all in the welding

zone by separating the blanks, shown in **Fig. 4 (C-E)**. The two pictures at the left are results of quasi-static tests with failure in the welding zone (**Fig. 4, A**) and failure in the aluminum flyer marked by the arrow (**Fig. 4, B**).
For the steel-aluminum joint peel tests a modified test setup was chosen, as the DP1000 did not allow the bending procedure as used for the aluminum samples. The aluminum flyer was loaded by a rotating slotted bolt that fits into the gap between the joint blanks (**Fig. 5**, **A**). The aluminum flyer sheet was inserted through the slit in the bolt. The bolt had a hexagon socket head to introduce rotational loading. The tests were performed comparable to DIN EN ISO 10447.

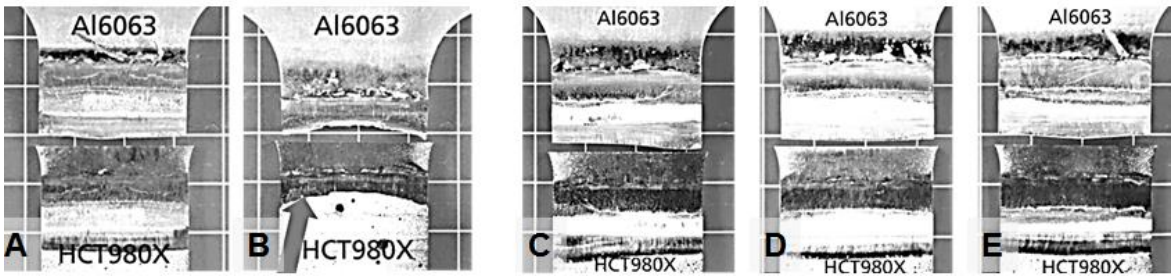

Figure 4: *Failed lap-shear samples with different failure modes at 0.02 m/s (A and B) with reproducible failure mode in the welding zone at 3 m/s loading speed (C-E). The view is on the welded sides of the blank, the contact surfaces.*

The failure modes for this loading situation scatter from pure welding zone failure (**Fig. 5 B**) with different mixed failure modes (**Fig. 5, C and D**) to a pure aluminum flyer failure (**Fig. 5 E**).

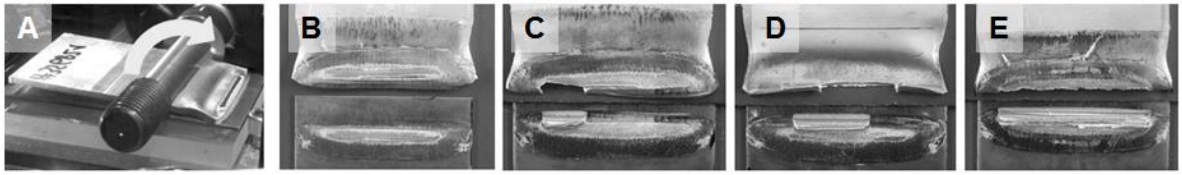

Figure 5: M*odified peel test setup (A), series of failed peel test samples (B-E) with the DP1000 (HCT980X) target (lower part) and the failed EN AW-6063 flyer (upper part); peel test failure modes of the mixed joint under monotone rotational load until failure, looking at the contact surfaces of the blanks*

4 Fatigue Testing and Assessment

Peel and lap shear tests were conducted with oscillating loads for aluminum and mixed steel-aluminum samples, too, **Tab. 1**. In these fatigue tests a cyclic axial load was applied to the specimen with a load ratio $R = F_{min}/F_{max}$ of R = 0 using load control. For the peel specimens a second load ratio of R = 0.5 was used to investigate the sensitivity to mean

stress. The testing frequency was set to f = 20 Hz. All tests are performed until rupture of the specimen or until a maximum number of load cycle N = 10^7 cycles was reached. Details for the EN-AL 6016- EN-AL 6016 samples are discussed in Baumgartner, J., Schnabel, K., Huberth, F. (2017).

Specimen type	Material	R	Failure
Peel	Al-Al	0, 0.5	Al. base metal
Shear	Al-Al	0	Al. base metal
Peel	Al-St	0	Al. base metal
Shear	Al-St	0	St. base metal / joint region

Table 1: *Overview on the fatigue tests*

In **Fig. 6** the results for the lap-shear tests of the mixed aluminum-steel samples are shown. As the failure occurred in the aluminum base metal not in vicinity of the joint, a second geometry was introduced to increase the stresses in the welding zone. For this reason the net section was reduced in the welding zone, as sketched in Fig. 6 in the corner.

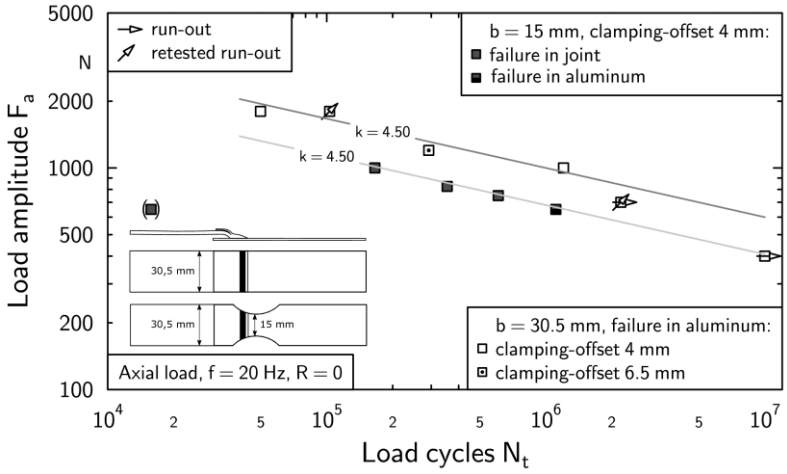

Figure 6: *Experimental results for lap-shear tests at cyclic axial load at 20 Hz, R=0 for mixed EN AW-6063-DP1000 samples with two geometries, sketched in the diagram*

For a fatigue assessment FE-models have been set up for all specimen types. In these models, the failure critical notches have been rounded with a reference radius of r = 0.05 mm in order to apply the notch stress approach. All FE-models have been validated using the results from an experimental strain analysis.
By using the fatigue test data and the numerically derived notch stresses, endurable notch stresses could be derived. A comparison of these stresses with endurable stresses taken from investigations on conventional aluminum laser beam welded overlap joints (Störzel 2011) showed a good agreement, **Fig. 7**. A comparison of the derived endurable notch stresses with design S-N curves from literature (FAT200 for Al-Al joints and FAT630 for St-St joints, (DVS Merkblatt 0905)) shows a good agreement. All besides on single test data is position over the according design S-N curve. This indicates a conservative assessment for such type of joints.

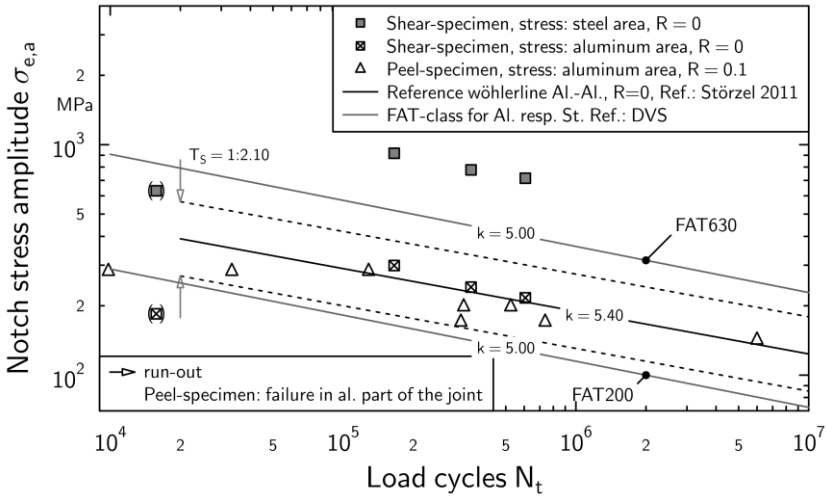

Figure 7: R*esults for lap-shear tests at cyclic axial load for mixed EN AW-6063-DP1000 samples, two geometries compared to the reference S-N-curve Al.-Al. and the FAT 200 for Aluminum as well as the FAT 630 for Steel according to the German Welding Society (DVS)*

5 Modelling and Crash Simulation

The modelling of the EMPT-welding zone and the samples was performed in three steps shown in **Fig. 8**.

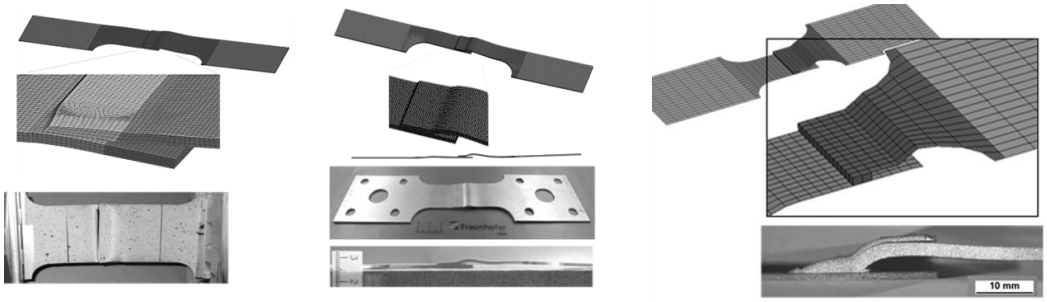

Figure 8: *Variants of the coupon test modelling, detailed solid model (left), shell model for aluminum samples (center) and the mixed samples (right) with corresponding real samples below each variant*

For the aluminum samples a detailed solid element model variant was used as reference with connected nodes in the welding zone. As a second step a computationally efficient shell based model with cohesive elements for the joint was applied, which is typically used in crash modelling. This modelling concept with shells was transferred to the mixed samples and adapted to the specific geometry of the coupon tests. For the base materials the strain rate dependences were applied.

5.1 Component Testing and Simulation

As mentioned above, the EMPT was used to join a mixed steel-aluminum T-joint component with a bended DP1000 U-profile and a machined EN-AW-6063 extrusion profile with two side flanges attached on the U-profile by 2 joints per flange (**Fig. 9**, left).

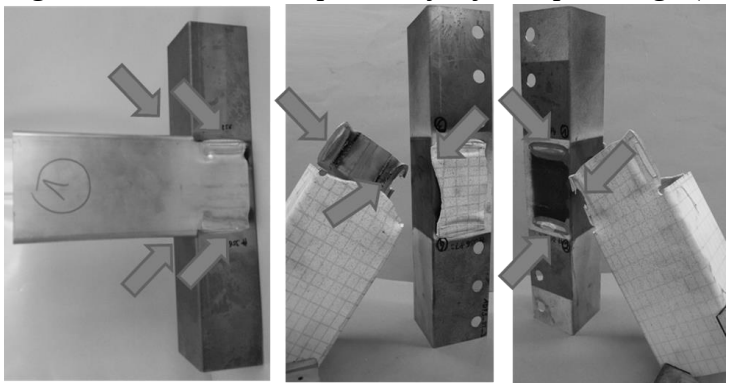

Figure 9: *EMPT-joined component "T-joint" before testing (left) with 4 welding zones, 2 at each flange, marked by the arrow and one part after testing, 2 views (middle and right) showing the mixed failure ranging from debonding or partial debonding to flange failure.*

These EMPT-joined components were tested under impact loading at about 6.5 m/s impactor velocity. The impactor velocity and the axial forces were measured. All tests were filmed with high speed video cameras, such that all welding zones were observed during the tests. Based on the coupon results the impact tests were modelled and simulated with different mixed joining zone areas, as measured on the failed samples, ranging from 89 mm^2 to 278 mm^2. Two examples are shown in comparison to measured forces and displacement of the impactor tests in **Fig. 10**. These examples show an average result (simulation 14, left) as well as a high force level result (simulation 15, right). For the result shown in **Fig. 10** on the right, the failure mode in the simulation is shown in **Fig. 11**. For comparison a test result with the initial failure occurring at the upper welding zones taken from the high speed video is shown in **Fig. 12** with comparable failure modes.

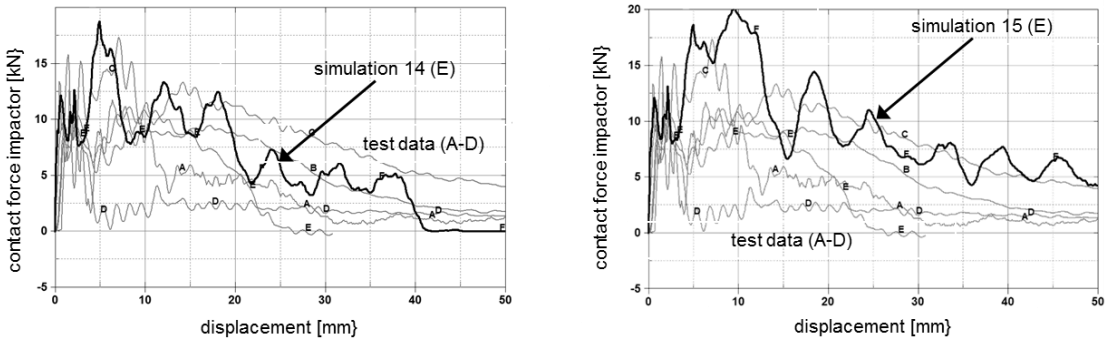

Figure 10: *Test results compared to impact simulation results for the T-joined component; the experimental results show a large scatter as shown for the failure (**Fig. 9**). The simulation results were calculated with different welding zone areas: at the left (simulation 14) with 222 mm² and 89 mm², non-symmetric, at the right (simulation 15) with 278 mm² and 167 mm², non-symmetric.*

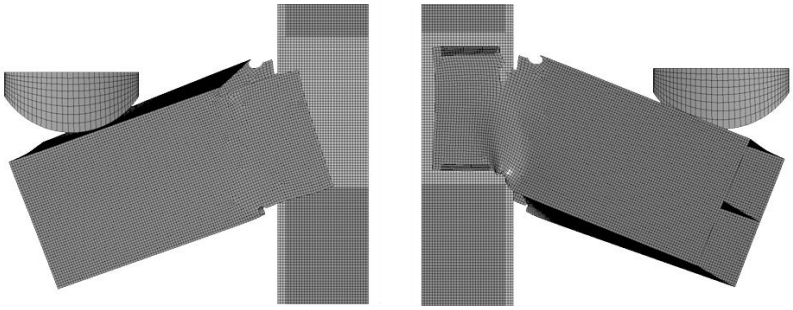

Figure 11: *Failure for simulation variant 15 with 278 mm² and 167 mm²joining area, non-symmetric: mixed failure with flange debonding (left) on one side and flange tear off (right) on the other side of the component; (corresponding force displacement is shown in* **Fig.10***, right, curve simulation 15 E)*

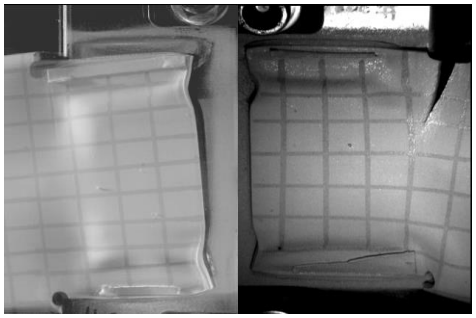

Figure 12: *Failure of the T-joint sample corresponding to the simulation variant 15 with 278 mm² und 167 mm²joining area, non-symmetric: mixed failure with flange debonding (left) on one side and flange tear off (right) on the other side of the component; (corresponding force displacement see* **Fig.10***, test data curve C)*

6 Conclusions

The final component tests reveal the problem of the scatter in failure loads and failure modes and the resulting scatter for the load bearing capacity of the component on the one hand, but also the high potential of the EMPT joining process for mixed material metal structures in light weight automobile body applications. The process of characterization and modelling was successfully introduced and the transferability of coupon test based parameters to a component demonstrated. The component tests with the resulting failure by flange tear off clearly indicate the potential of the EMPT joining process to overcome the general problem of weakening in the bonding area, as discussed in the introduction.
For the fatigue analysis the notch stress approach was successfully applied. A comparison of the endurable stress levels with results from investigations on conventional aluminum laser beam welded overlap joints showed the competitiveness of the EMPT joining process.

Combined with improved reproducibility and an EMPT optimized construction, this technology offers a high potential for mixed materials light weight structures.

Acknowledgments

The presented investigations were supported by financial funding from the Federal Ministry of Economics and Technology BMWi via the AiF e.V. (Arbeitsgemeinschaft industrieller Forschungsvereinigungen "Otto von Guericke" eV) under the grant 17.883N. Technical and scientific support during the project was given by the Germany Welding Society (DVS eV) and the industrial steering committee. The authors would like to thank the AiF, the DVS, and the members of the steering committee for their support.

References

Meschut, G., Janzen, V. & Olfermann, T., 2014, Innovative and Highly Productive Joining Technologies for Multi-Material Lightweight Car Body Structures. Journal of Materials Engineering and Performance (2014) 23: 1515. https://doi.org/10.1007/s11665-014-0962-3

Kang, B.-J., 2015, Review of magnetic pulse welding; Journal of Welding and Joining, Vol.33 No.1 (2015) pp7-13, http://dx.doi.org/10.5781/JWJ.2015.33.1.7

Poll, D., 2017, Neue A8-Karosse besteht erstmals aus vier Werkstoffen, https://www.produktion.de/bildergalerien/neue-a8-karosse-besteht-erstmals-aus-vier-werkstoffen-101.html, 05/2017

Huberth, F., Baumgartner, J., 2017, Schlussbericht zu IGF-Vorhaben Nr. N17883 N/1, Versagensverhalten von Mischschweißverbindungen unter mehrachsiger crashartiger und schwingender Beanspruchung am Beispiel von EMPT-Blechschweißungen, Freiburg/ Darmstadt 2017

DIN EN ISO 10447:2015-05, Widerstandsschweißen - Prüfung von Schweißverbindungen - Schäl- und Meißelprüfung von Widerstandspunkt- und Buckelschweißverbindungen (ISO 10447:2015); Deutsche Fassung EN ISO 10447:2015

Baumgartner, J., Schnabel K., Huberth, F., 2017, Fatigue assessment of EMPT-welded joints using the reference radius concept, 7th International Conference on Fatigue Design, Fatigue Design 2017, 29-30, November 2017, Senlis, France

Störzel, K., Baumgartner, J., Bruder, T., Hanselka, H., 2011 Festigkeitskonzepte für schwingbelastete geschweißte Bauteile, Materials Testing 53 (2011) 418–426. doi:10.3139/120.110244.

DVS Merkblatt 0905 - Industrielle Anwendung des Kerbspannungskonzeptes für den Ermüdungsfestigkeitsnachweis von Schweißverbindungen DVS - Deutscher Verband für Schweißen und verwandte Verfahren e.V., DVS - Deutscher Verband für Schweißen und verwandte Verfahren e.V., 2017